A Continuously Variable Transmission System Designed for Human-Robot Interfaces

Emir Mobedi and Mehmet İsmet Can Dede
Mechanical Engineering Department, Izmir Institute of Technology
Email: {emirmobedi, candede}@iyte.edu.tr

Abstract

Continuously Variable Transmission (CVT) systems are being used for many applications such as automotive transmissions, robotics, aerospace. In an ideal condition, these systems have the potential to provide continuously varying power transmission within a predefined limit. This transmission is accomplished with the help of friction, belt or gear systems. CVT can find application in a human-robot interface if design criteria such as backdrivability, independent output position and impedance variation, shock absorbing and low mass and inertia can be satisfied. Even if there are various CVT designs in the literature for human-robot interfaces, the primary limitation of the two-cone drive CVT designs is that the output torque and the output position cannot be altered independently. The reason for this problem is that the friction wheel, which is designed to transmit the torque from the input cone to the output cone, gives rise to remarkable longitudinal friction force along the linear way. In order to overcome this problem, a sphere is used in this work for the CVT design as the transmission element. In addition, it is stated in the literature that common CVT drive systems do not have the capability to be used in cyclic bidirectional motion. In the presented CVT design, a second sphere is added to the system with two springs from the lower part of the cones for pre-tension in order to solve the bidirectional transmission problem. In this paper, the working principle and conceptual design details of the novel two-cone CVT drive are presented. Experimental results showed that the novel CVT has the capacity to transmit bidirectional power with some accuracy.

Keywords: Continuously variable transmission, Human-robot interaction, Haptics

1 Introduction

For many decades, robots' primary employment has been in industrial tasks such as polishing, welding, pick and place. They are developed to follow only the predefined trajectory with high position accuracy and they can be named as conventional industrial robots. Even if they had the capability to achieve some tasks, they were not allowed to work with the human operators' side by side. This limitation was due to the safety reasons as well as the absence of advanced sensory systems. As a consequence, the conventional industrial robots are confined in strictly defined working cells or workshops.

In recent years, a new generation of robots named collaborative robots has been produced to work alongside with humans in order to increase the efficiency of the work. The well-known examples are industrial coworkers and household robots. These robots are being developed under ISO 10218-1 standard in order to prevent any damage to the human coworker. First clause of this standard (5.10.1) defines a condition that no motion will be allowed if the operator is in the collaborative workspace. In the second

clause (5.10.2), the robot can be moved as long as the operator gives direct force input to the robot. The next clause (5.10.3) is related to the distance defined between the human and the robot. The operation can be achieved if this distance is not exceeded. In final clause (5.10.5), robots having inherent force limiting are allowed to work with human operators in continuous contact because they are not capable of applying excessive forces to the operator. This task can be achieved by control design, mechanical design or combination of them. The CVT presented in this paper is designed as a mechanical solution for constructing the active joint structure of a robot by following the 4th part of the standard, which enables the user to work with the robot in continuous contact situation.

Considering the joint structures of collaborative robots, designers should consider some additional design criteria including backdrivability, mechanical impedance, workspace, low mass and inertia, variation of impedance without disturbing the motion, and shock absorbing [1]. Good backdrivability is achieved when the resistance of the robot to the motion input by the human from the end-effector is minimized [2]. When there is a physical interaction, the robot is expected to be backdrivable so that the human-robot interaction happens in a two-way stream. The aforementioned resistance is defined as mechanical impedance which relates the induced force to the subsequent velocity for a robot. It should be the maximum for enhancing accuracy and minimum for enhancing the backdrivability. Thus, the problem is narrowed down to the adjustment of the robot's impedance either mechanically or by control. A solution to this has been proposed by designing variable impedance actuators and joint structures.

Antagonistic springs with antagonistic motor type of joints are listed in the literature as variable impedance joints [3]. The primary advantage is that without the need of using a current control for the motor, joint stiffness and joint angle are changed independently from each other by the help of this mechanical stiffness device [4]. However, in this design, the workspace is limited because of the limits of the used servomotors.

Another design is antagonistic springs with independent motors [4]. In this setup, there are two motors which are used for stiffness variation and joint position variation. Accordingly, the mechanism is capable of altering the joint motion and stiffness independently. The device has shock-absorbing feature due to the spring located between the joint and the base. However, since stiffness motor is located at the joint, the joint structure's mass and inertia are increased. Therefore, backdrivability property is adversely affected.

Among the possible CVT designs, planetary gear based CVT drives are capable of altering the stiffness mechanically [5]. In addition, it is claimed that it is able to provide protection inherently against overloading. Also, the design is claimed to be simpler than spring-based variable-stiffness joints. Hence, it is easy to carry out the force and kinematic analysis of the system. On the other hand, stiffness and position cannot be altered independently as one of the inputs of the system is output resistance. In addition, since the mechanism is produced with the planetary gear system, the inertia of the gears increases the inertia felt by the user in addition to the increased friction effects while backdriving the system from the end-effector.

Another well-known CVT drive is developed by the use of dry friction. The first robot that uses this working principle, Cobot [6], was designed for haptic applications. In this design, there are CVT wheels, which are coupled with the proximal link and the

power cylinder. When stiffness variation is required, the power cylinder is rotated and CVT wheels are steered depending on the desired stiffness. Therefore, stiffness variation is achieved by altering the angle between the power cylinder and CVT wheels. However, the power cylinder makes the design bulky because of its footprint. Spherical continuously variable transmission (S-CVT) is yet another CVT design example [7]. In S-CVT system, two input discs, two output discs and one variator having friction surfaces are connected with a sphere in order to adjust the stiffness of the output discs by the help of friction force. Input and output discs have point type of contact with the sphere. By adjusting the location of the rotation axis of the sphere, output velocity and output torque are altered.

Finally, CVT cone drives are used to change the output torque in a continuous way. In this drive system, two cones are located parallel to each other. The transmission between the cones is realized with the help of dry friction, belt or gear [8]. Two problems are detected in the literature related to dry-friction two-cone drive systems. Firstly, the transmission occurs only in one way and output torque cannot be changed without altering the output position. These issues limit the usage of two-cone CVT systems for the human-robot interface. Hence, in this study, the working principle, conceptual design details and experimental validation results of a new two-cone CVT drive system are presented to propose a solution to the aforementioned problems.

2 Working Principle of the Novel CVT

In this section, the working principle of the novel CVT is presented. In conventional friction-drive two-cone CVTs, there are two cones which are covered with friction material and a wheel is used to transmit the moment from one cone to the other. Moment and speed transmission levels are altered by changing the ratio of the radii between the input and output cones by varying the point of contact of the wheel. However, it is not possible to control output position and output torque independently in this way since the wheel does not have the capability to perform the holonomic motion. In other words, cones must be rotated to change the transmission ratio and this situation limits the usability of the two-cone CVT drive in human-robot interfaces. To cope with this issue, the first modification is made by using a sphere, which is capable of executing holonomic motion (Figure 1). Hence, point type of contact with two cones is guaranteed which allowed controlling output position and output torque independently. Also, the cones are covered with a rubber used diaphragm to create friction surfaces on the cones to avoid slippage without applying the larger amount of normal force on the cones. At this point, a limitation of the continuously variable transmission system should be mentioned. This limitation occurs because the sphere and the cone form a point-type of contact for ideally rigid structures. As a result of this, the transmitted torque is limited. However, in the application, neoprene material is used for the friction surface which was also used in HAPKIT for constructing the friction drive [9]. The use of this soft material changes the contact type from an ideal point-type of contact to an ellipse-shaped contact. This ellipse-shaped contact area enlarges with respect to the applied normal force creating a larger contact surface. In this way, the aforementioned limitation on the limitation of the torque transmission is avoided.

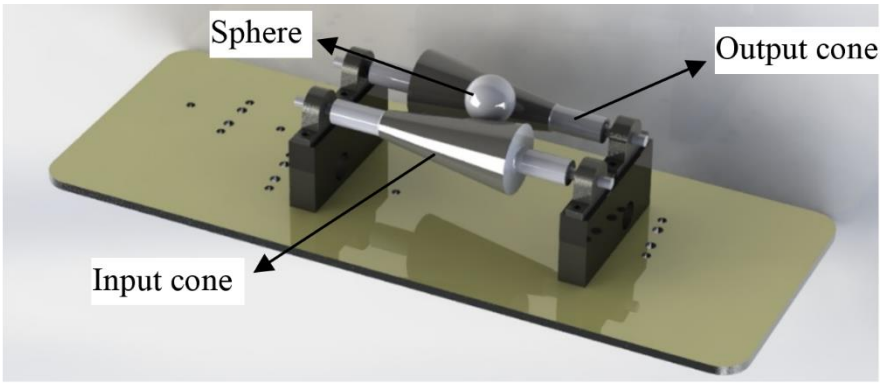

Figure 1: Isometric view of the single-sphere two-cone CVT

The location of the spheres is important for the shifting action which accomplishes alteration of the transmission ratio. If the sphere is located exactly between two cones, it is not possible to change the transmission ratio without changing the output position. The mathematical proof of the reason is presented as follows;

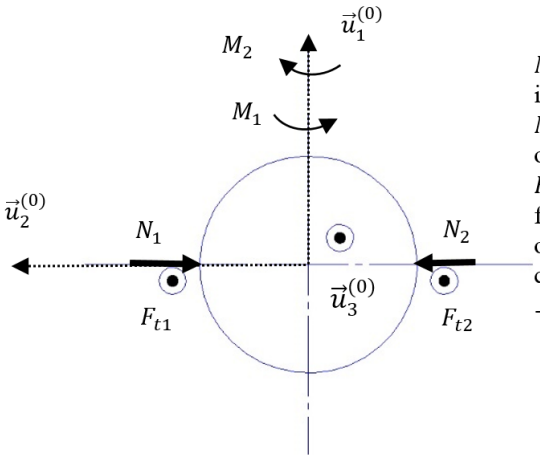

N_1: Normal force applied by the input cone
N_2: Normal force applied by the output cone
F_{t1} & F_{t2}: Tangential friction forces acting on the left & right side of the sphere in the opposite direction of the shifting force along $-\vec{u}_3^{(0)}$

Figure 2: Free-body diagram of the sphere located between the cones

$$\vec{M}_1 = r\vec{u}_2^{(0)} \times F_{t1}\vec{u}_3^{(0)} = F_{t1} r\vec{u}_1^{(0)} \quad (1)$$
$$\vec{M}_2 = -r\vec{u}_2^{(0)} \times F_{t2}\vec{u}_3^{(0)} = -F_{t2} r\vec{u}_1^{(0)} \quad (2)$$

Tangential forces are equal to each other since the normal forces and friction coefficient are the same for the two cones. Therefore, the sphere cannot roll around the $\vec{u}_1^{(0)}$ axis and it needs to slip between the two cones in order to change the transmission ratio. However, slip between the cones and the transmission element is not desired in order to guarantee the transmission within the selected limit value of applied torques from the input cone. For this reason, the sphere should be able to roll instead of a pure slippage and thus, it is located above the cones. The mathematical proof of the rolling

action of the sphere is shown by the following equations based on the free-body diagram of the sphere located above the cones presented in Figure 3;

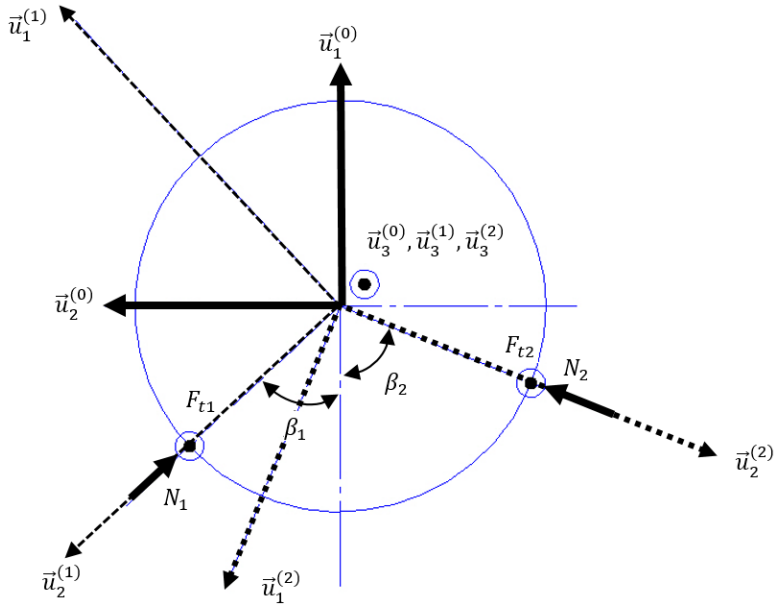

Figure 3: Free-body diagram of the sphere located above the cones

The angle between the frames $\mathcal{F}_0$ and $\mathcal{F}_1$ and $\mathcal{F}_0$ and $\mathcal{F}_2$ are defined as $\sphericalangle\, \vec{u}_1^{(0)} \rightarrow \vec{u}_1^{(1)} = \frac{\pi}{2} - \beta_1$; $\sphericalangle\, \vec{u}_1^{(0)} \rightarrow \vec{u}_1^{(2)} = \frac{\pi}{2} + \beta_2$. Based on this definition, the moments that the friction forces in the opposite direction of the shifting force are calculated as follows:

$$\vec{M}_1 = r\vec{u}_2^{(1)} \times F_{t1}\vec{u}_3^{(1)} = F_{t1} r \vec{u}_1^{(1)} \qquad (3)$$
$$\vec{M}_2 = r\vec{u}_2^{(2)} \times F_{t2}\vec{u}_3^{(2)} = F_{t2} r \vec{u}_1^{(2)} \qquad (4)$$

The above vector equations can be resolved in the inertial frame $\mathcal{F}_0$ as presented in Equations 5 and 6. It should be noted that; $\hat{C}^{(0,i)}$ is the transformation matrix between the inertial frame and the i[th] frame, $\tilde{u}_3$ resembles the skew symmetric matrix form of the $\bar{u}_3$ column matrix.

$$\bar{M}_1^{(0)} = \hat{C}^{(0,1)} \bar{M}_1^{(1)} = F_{t1} r e^{\tilde{u}_3 (90 - \beta_1)} \bar{u}_1 = F_{t1} r [\bar{u}_1 \sin\beta_1 + \bar{u}_2 \cos\beta_1] \qquad (5)$$
$$\bar{M}_2^{(0)} = \hat{C}^{(0,2)} \bar{M}_2^{(2)} = F_{t2} r e^{\tilde{u}_3 (90 + \beta_2)} \bar{u}_1 = F_{t2} r [-\bar{u}_1 \sin\beta_2 + \bar{u}_2 \cos\beta_2] \qquad (6)$$

When Equations 5 and 6 are investigated, it is obvious that $\vec{u}_2$ component of the moments allows the sphere to roll on the cones and $\vec{u}_1$ component of the moments act against each other prevent the rotation around $\vec{u}_1$. Therefore, it is possible to move the transmission element without the necessity of slippage and this is the reason why the sphere must be located above the cones.

Nevertheless, relocation of the sphere above the cones does not solve the problem fully. In order to explain the new problems, Figure 4 and 5 are sketched. In Figure 4, it is assumed that there is a handle coupled with the output cone and the user holds it. When the input is in CW direction, the transmission is achieved as indicated in Figure 4. The friction forces acting on the sphere during transmission is the downward direction (P_1, P_2) and hence, the transmission without slippage is guaranteed up to a certain limit. For the other case in which the input is in CCW direction as presented in Figure 5, transmission cannot be guaranteed since the friction forces acting on the sphere (P_3, P_4) are upward and this reduces the normal force between the sphere and cones ("W" is the weight of the sphere). This situation can result in slippage at the point of contact at lower torque transmission limits. In order to deal with this problem, we propose adding a second sphere below the cones. Also, as presented in Figure 6, two forces are used to apply pre-tension (F_1, F_2) to each sphere in order to solve the bidirectional transmission problem.

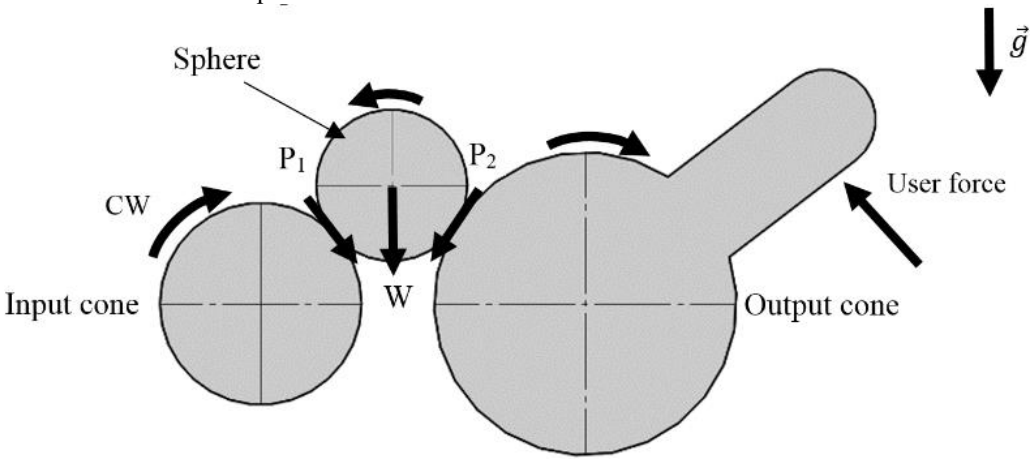

Figure 4: Side view of the one sphere CVT in CW direction

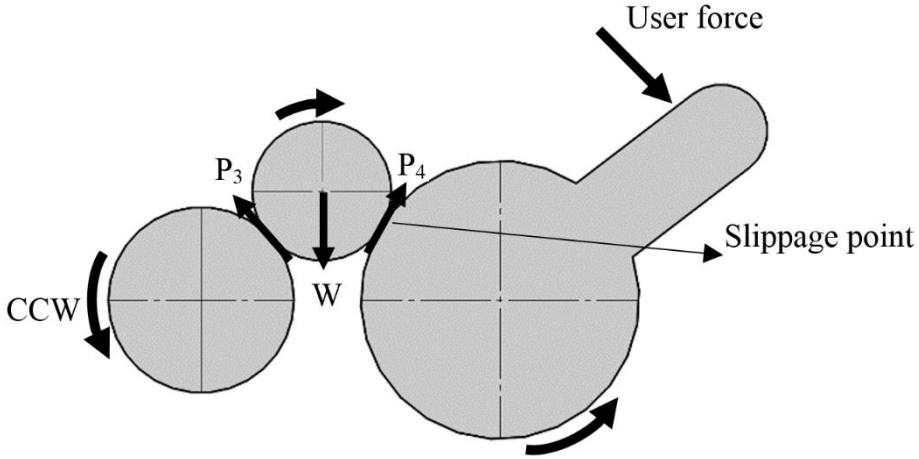

Figure 5: Side view of the one sphere CVT in CCW direction

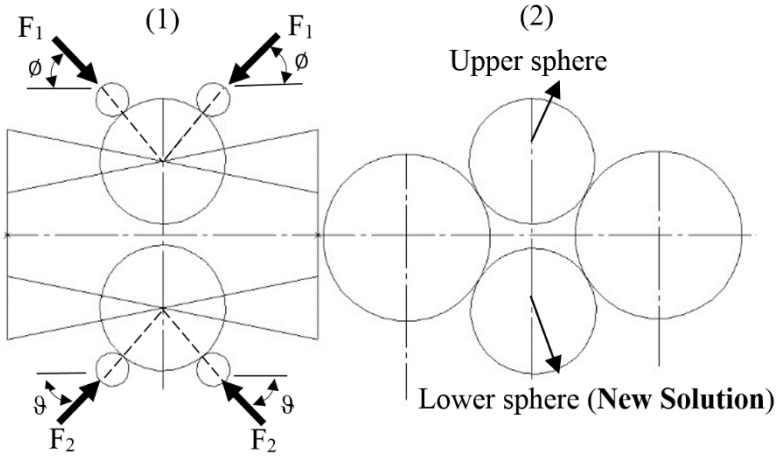

Figure 6: (1) Front view of the system (2) Side view of the system

3 Proof of the Concept Design

The design details of the novel CVT are presented in this section in order to be used for manufacturing a prototype for proof of the design tests.

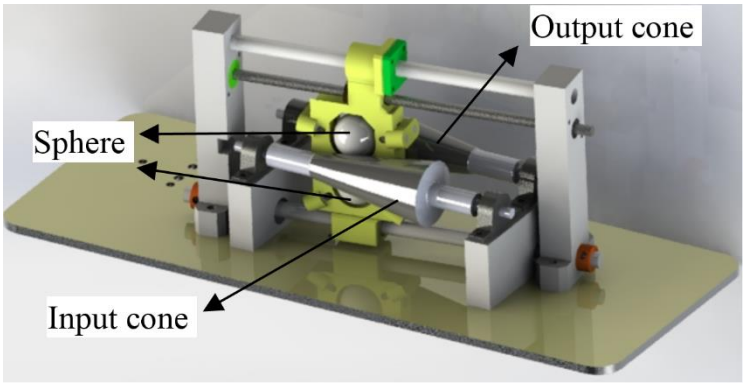

Figure 7: Isometric view of the double-sphere two-cone CVT

First, the exploded view of the carriage system, which is used to carry the two spheres that alter the transmission ratio, is indicated in Figure 8.

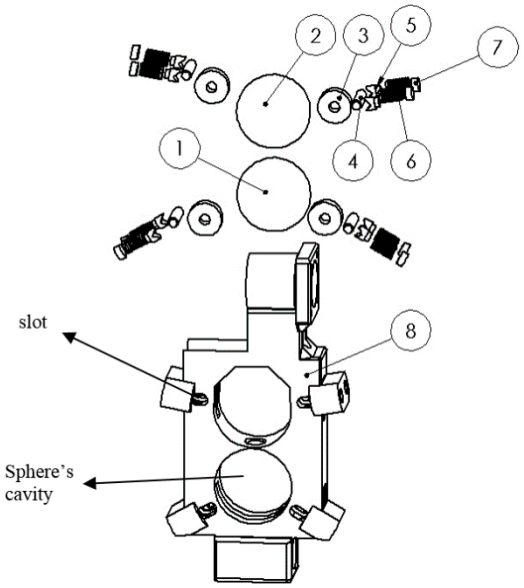

Figure 8: Exploded view of the carriage system

In this design, there are total of 8 parts as follows: compression springs **(6)**, support elements **(5)**, 4 pieces of steel pins **(4)** and bearings **(3)**, 2 pieces of steel spheres **(1,2)** and the carriage **(8)**. In the assembly process, first, upper and lower spheres are placed into the sphere cavities and the bearings are placed into the slots. Later, steel pins are mounted through the inner rim of the bearings so that the spheres can be confined in the carriage. The next step is related to the application of pre-tension on the spheres. Two support elements are located at the back of the steel pins and springs are placed at back to the aforementioned support elements. Finally, a set-screw is mounted on the spring so that the pretension of the spring can be altered. After assembling the carriage system, the carriage system is assembled on a screw-nut **(11)** and linear guides **(9)** at the upper and lower part of the carriage system as shown in Figure 9. The cones are denoted as **(10)** and the bedding pieces for the cones and the carriage's linear guides are denoted as **(12)** and **(13)** respectively.

By adjusting the normal force between the cones and sphere through varying the compression on springs denoted by **(6)**, the torque limits can be set. As an example; if it is required to set the torque transmission limit to lower values, the normal force is reduced by releasing the compression on the spring and as a result of this, when this limit is exceeded, there will be slippage between the cones and the sphere. This property enables protection from the excessive amount of torques to be applied either to the user or to the actuator during operation. Therefore, the joint structure is inherently safe in the mechanical design sense.

If the system is arranged so that the spheres are aligned along the vertical axes then, the compression force (F_2) on the below sphere has to be higher than the compression force (F_1) on the above sphere in order to overcome the gravitational effects. As a result of this adjustment, normal forces between the cones and the spheres are set to be equal to each other, and the same type of transmission in two directions is made possible.

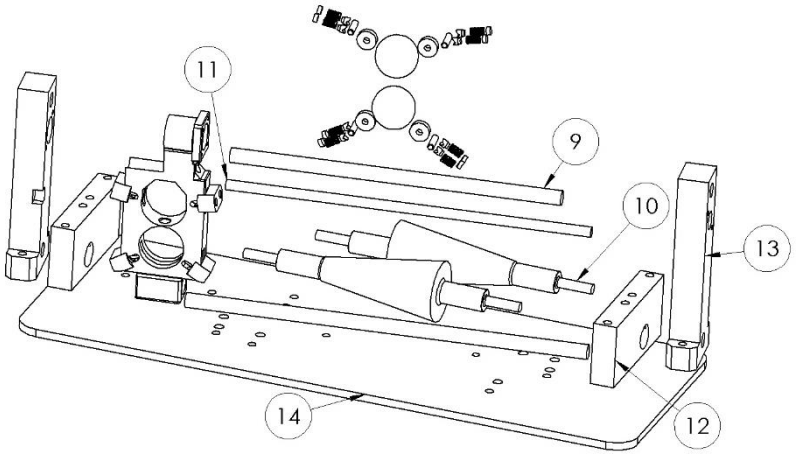

Figure 9: Exploded view of the whole assembly

The reason why bearings are used to transmit the compression force to the spheres is to minimize the friction during linear guiding, which results in quicker response time for the variations in the transmission ratio.

4 Experimental Results

In order to validate the proof of concept design, an experiment is conducted to observe if the same amount of torques can be transmitted in both directions; CW and CCW. The experiment is carried out by determining 6 locations of the cone that corresponds to different test diameters. The selected locations' diameters are measured on the cones by the help of digital caliper (Mitutoyo). Input torque of 72 mNm is applied by hanging a calibrated mass on the input cone from a measured moment arm length. An encoder (Figure 10) with 0,3515625° resolution is assembled on the input cone to observe if any slippage occurs between the input cone and the sphere. Output cone is coupled with a force/torque sensor (ATI, Nano17), which is presented in Figure 11, in which only the torque along the axis of rotation of the cone is measured. The output cone is mechanically fixed to the inertial frame in order to constrain its rotation. The results are presented as follows;

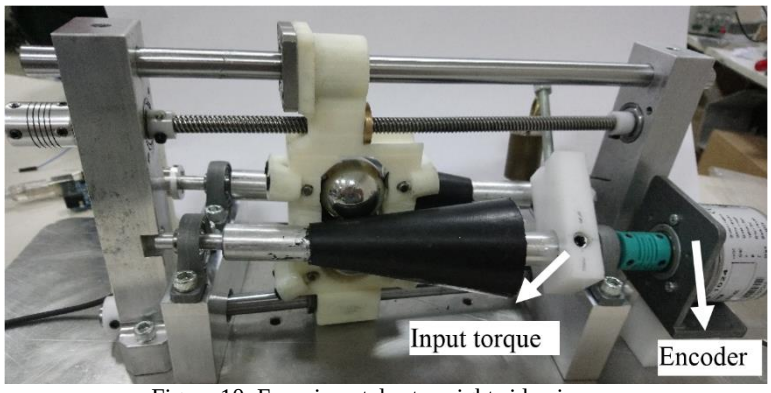

Figure 10: Experimental setup right side view

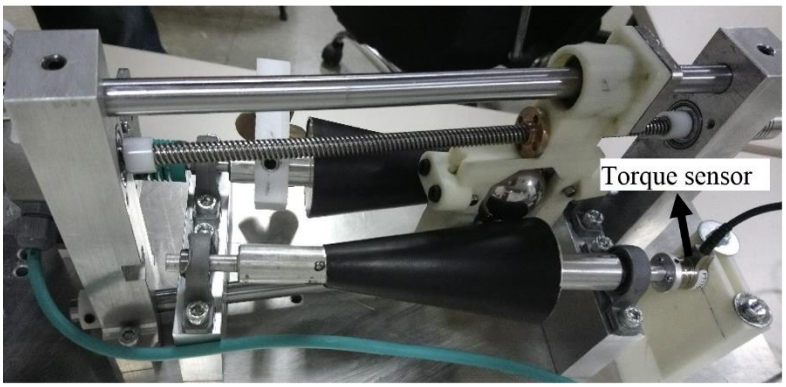

Figure 11: Experimental setup left side view

Table 1. Experimentally obtained output torque results

r_{out}/r_{in}	Input torque(mNm)	Direction	Output torque (mNm)
0.56	72	CW CCW	33.39 32.22
0.75	72	CW CCW	40.17 43.36
0.95	72	CW CCW	52.52 51.98
1.07	72	CW CCW	66.57 65.17
1.31	72	CW CCW	68.21 73.80
1.36	72	CW CCW	85.66 80.40

In Table 1, the output torques for the same input torques in both CW and CCW directions are measured for each test point. According to these results, the torque transmission in both directions was accomplished.

Nevertheless, there are relatively small inconsistencies between the output torque measured CW and CCW directions at the same test point. Also, the inconsistency between the direction of operation is not always in the favor of one direction. For example, the CW output torque is higher than the CCW only in the 1st, 3rd, 4th and 6th test locations. Therefore, it can be concluded that the inconsistency is not due to the concept that is tested here but due to the measurement inconsistencies and manufacturing errors. Especially, the manufacturing errors affecting the smoothness of the surfaces and the errors when placing the friction surfaces on the cones may have affected these results.

5 Conclusion

In this study, a new continuously variable transmission system to be used for human-robot interaction is introduced. The primary novelty of the design presented in this work is the modification of the transmission element from a wheel to two spheres. The experimental results with the proof of concept prototype have showed that bidirectional torque transmission was made possible with this design. Also, with this design, the user is able to alter the backdrivability level by ensuring safe physical interaction which is one of the most critical issues of the human-robot interfaces. As a future work, the proposed design will be optimized to be used for haptic device designs for varying the impedance range of the device.

Acknowledgments
This work is supported in part by The Scientific and Technological Research Council of Turkey via grant number 117M405.

References

1. S. Wolf, G. Grioli, O. Eiberger, W. Friedel, M. Grebenstein, H. Höppner, E. Burdet, D. G. Caldwell, et al., “Variable Stiffness Actuators: Review on Design and Components,” IEEE Transactions on Mechatronics, 21(5), 2016, 2418-2430.
2. T. Ishida, A. Takanishi, “A Robot Actuator Development with High Backdrivability,” IEEE Conference on Automation and Mechatronics, 2006, 1-6.
3. S. A. Migliore, E. A. Brown, S. P. DeWeerthgn “Biologically Inspired Joint Stiffness Control,” ICRA Proceedings of the IEEE International Conference on Robotics and Automation, 2005, 4508-4513.
4. B. Vanderborght et al., “Variable Impedance Actuators: A review,” Journal of Robotics and Autonomous Systems, ICRA Proceedings of the IEEE International Conference on Robotics and Automation, 2013, 1601-1614.
5. K. S. Ivanov, G. Ualiev, B. Tultaev, “Kinematic and Force Analysis of Robot with Adaptive Electric Drives,” Applied Mechanics and Materials, Journal of Robotics and Autonomous Systems, 555, 2014, 273-280.
6. E. L. Faulring, J. E. Colgate, M. A. Peshkin “The Cobotic Hand Controller: Design, Control and Performance of a Novel Haptic Display,” The International Journal of Robotics Research, 25(11), 2006, 1099-1119.

7. J. Kim, “Design and Analysis of a Spherical Continuously Variable Transmission,” Journal of Mechanical Design, 124(1), 2002, 21-29.
8. N. Sclater, N. P. Chironis, Mechanism and Mechanical Devices Sourcebook: The McGraw-Hill Companies, 2001.
9. M. O. Martinez, T. K. Morimoto, A. T. Taylor et al., “3D Printed Haptic Devices for Educational Applications,” IEEE Haptics Symposium, 2016, 126-133.